Purely irrotational theories for the viscous effects on the oscillations of drops and bubbles

J.C. Padrino [a], T. Funada [b] and D.D. Joseph [a,*]

[a] *Department of Aerospace Engineering and Mechanics, University of Minnesota, 110 Union Street SE, Minneapolis, MN 55455, USA*

[b] *Department of Digital Engineering, Numazu College of Technology, Ooka 3600, Numazu, Shizuoka, 410-8501, Japan*

Abstract

In this paper, we apply two purely irrotational theories of the motion of a viscous fluid, namely, viscous potential flow (VPF) and the dissipation method to the problem of the decay of waves on the surface of a sphere. We treat the problem of the decay of small disturbances on a viscous drop surrounded by gas of negligible density and viscosity and a bubble immersed in a viscous liquid. The instantaneous velocity field in the viscous liquid is assumed to be irrotational. In VPF, viscosity enters the problem through the viscous normal stress at the free surface. In the dissipation method, viscosity appears in the dissipation integral included in the mechanical energy equation. Comparisons of the eigenvalues from VPF and the dissipation approximation with those from the exact solution of the linearized governing equations are presented. The results show that the viscous irrotational theories exhibit most of the features of the wave dynamics described by the exact solution. In particular, VPF and DM give rise to a viscous correction for the frequency that determines the crossover from progressive to standing waves. Good to reasonable quantitative agreement with the exact solution is also shown for certain ranges of modes and dimensionless viscosity: For large viscosity and short waves, VPF is a very good approximation to the exact solution. For small viscosity and long waves, the dissipation method furnishes the best approximation.

Key words: drops, bubbles, potential flow, two-phase flow, gas-liquid flow, viscous potential flow.

* Corresponding author. Tel.: +1 612 625 0309; fax: +1 612 626 1558.
Email address: joseph@aem.umn.edu (D.D. Joseph).

1 Introduction

A viscous liquid drop surrounded by a quiescent gas or a gas bubble immersed in a viscous liquid tends to an equilibrium spherical shape if the effects of surface tension are significantly large in comparison with gravitational effects. When the spherical interface of the bubble or drop is slightly perturbed by an external agent, the bubble or drop will recover their original spherical configuration through an oscillatory motion of decreasing amplitude. In the case of the drop, depending upon its size and physical properties, the return to the spherical shape may consist of monotonically decaying standing waves. For a drop immersed in another viscous liquid, decaying oscillatory waves always occurs at the liquid-liquid interface.

Early studies on the subject for inviscid liquids are due to Kelvin (1890) and Rayleigh (1896). Lamb (1881) considered fully viscous effects on the oscillations of a liquid spheroid. The effect of viscosity on the rate of decay of the oscillations of a liquid globe was approximated by Lamb (1932) assuming an irrotational velocity field using the dissipation method. This result is independent of the nature of the forces that drive the interface to the spherical shape. Chandrasekhar (1959) studied fully viscous effects on the small oscillations of a liquid globe with self-gravitation forces neglecting surface tension. The same form of the solution was also obtained by Reid (1960) when surface tension instead of self-gravitation is the force that tends to maintain the spherical shape. A good account of both solutions is presented in the treatise by Chandrasekhar (1961). Following Lamb's reasoning, Valentine, Sather & Heideger (1965) applied the dissipation method to the case of a drop surrounded by another viscous liquid.

Comprehensive analyses of viscous effects in a drop embeded in liquid were presented by Miller & Scriven (1968) and Prosperetti (1980a) using normal modes. The latter found a continuous spectrum of eigenvalues for an unbounded outer fluid. Prosperetti (1977, 1980b) considered the initial-value, fully-viscous problem posed by small perturbations about the spherical shape of a drop or a bubble with no assumption about the form of the time dependence. The solution showed that the normal mode results are recovered for large times.

Finite size disturbances have received some attention. Tsamopoulos & Brown (1983) considered the small-to-moderate-amplitude inviscid oscillations using perturbations methods. Lundgren & Mansour (1988) and Patzek *et al.* (1991) studied the inviscid problem posed by large oscillations applying the boundary-integral and the finite-element methods, respectively. Lundgren & Mansour also investigated the effect of a 'small' viscosity on drop oscillations. Basaran (1992) carried out the numerical analysis of moderate-to-large-amplitude axisymmetric oscillations of a viscous liquid drop.

In this paper, approximate solutions of the linearized problem for small departures from the spherical shape for a drop surrounded by a gas of negligible density and viscosity or a bubble embedded in a liquid are sought using viscous potential flow (VPF) and the dissipation method. VPF is a purely-irrotational-flow theory in which viscosity enters the problem through the viscous normal stresses at the the interface (Joseph & Liao 1994a, 1994b, Joseph 2003). If the viscosities of the fluids are neglected, and only the irrotational pressure and capillary forces are included in the balance at the interface, the analysis reduces to inviscid potential flow (IPF). A viscous correction of VPF can be obtained by applying the dissipation method (Joseph & Wang 2004). In this approximation, which requires the evaluation of the mechanical energy equation, viscous effects are accounted for through the computation of the viscous dissipation

originated by the irrotational flow. In addition to his study of a viscous globule, the dissipation method was used by Lamb (1932) in his analysis of the effect of viscosity on the decay of free gravity waves. However, his analysis did not render viscous effects for the frequency of the waves. The dissipation calculation presented here does give rise to a viscous correction for the wave frequency, thus predicting a crossover from progressive to standing waves.

VPF was used by Funada & Joseph (2002) to study the problem of capillary instability. Their results were in much better agreement with Tomotika's (1935) exact normal-mode solution than inviscid potential flow. Wang, Joseph & Funada (2005a) computed the growth rates for this configuration by adding a pressure correction to VPF, when either the interior or exterior fluid is a gas of negligible density and viscosity. They found good agreement between their results and the exact solution. The case of capillary instability of two viscous liquids was considered by Wang, Joseph & Funada (2005b), obtaining good to reasonable agreement for the maximum growth rates whereas poor agreement for long waves. Wang *et al.* (2005a, 2005b) also used the dissipation method in the problem of capillary instability and obtained the same growth rate as the viscous correction of VPF. The decay of free gravity waves modeled as 'small' disturbances about an infinite plane free surface was studied by Joseph & Wang (2004) and Wang & Joseph (2006) using VPF and the pressure correction of VPF. They found that the rate of decay from VPF agrees with Lamb's exact solution for short waves, whereas the damping rate computed from the pressure correction of VPF for long waves agrees with both Lamb's dissipation result and his solution of the linearized Navier-Stokes equations. A comprehensive review on the theory of irrotational flow of viscous fluids was given by Joseph (2006).

Two viscous irrotational approximations are used in this study to determine the rate of decay and frequency of the oscillations on drops and bubbles, namely,

VPF or viscous potential flow, in which the viscosity enters the analysis through the viscous normal stress at the interface.

Dissipation method, which requires the integration of the mechanical energy equation with the approximation of irrotational motion yet zero-shear stress is satisfied at the free surface.

Results from these theories are compared to predictions from **IPF** or inviscid potential flow, in which the viscosity is set equal to zero, and the solution of the linearized incompressible Navier-Stokes equations using normal modes, hereinafter '**exact solution**', given in the literature.

This paper is organized as follows: First, VPF analysis of a drop embedded in a viscous liquid is presented and the limiting cases of a drop in vacuum and a bubble in liquid are obtained. In §3, the dissipation method is applied to the spherical shape. In §4, the exact solution of the linearized fully viscous problem is summarized. Results are discussed in §5 where several final remarks are presented.

2 Viscous potential flow analysis of a spherical drop immersed in another fluid

Consider a single spherical drop of radius a filled with a fluid with density ρ_l and viscosity μ_l immersed in another fluid with density ρ_a and viscosity μ_a. The coefficient of interfacial tension is denoted as γ. Both fluids are incompressible and Newtonian with gravity neglected. At the basic or undisturbed state both fluids are at rest and the pressure jump across the spherical interface is balanced by surface tension.

When the basic state is disturbed with small irrotational perturbations, the resulting velocity

field can be written as the gradient of a potential. The disturbance of the spherical interface is denoted by $\zeta \equiv \zeta(t, \theta, \varphi)$; the interface position is $r = a + \zeta$.

For irrotational flow the incompressible Navier–Stokes equations reduce to the Bernoulli equation. The resulting pressure field can be decomposed into the undisturbed pressure plus a 'small' disturbance.

After subtracting the basic state from the disturbed fluid motion and performing standard linearization of the resulting expressions by neglecting products of the small fluctuations and products of their derivatives, one obtains, for the interior motion ($0 \leq r < a$),

$$\nabla^2 \phi_l = 0, \tag{2.1}$$

$$p_l = -\rho_l \frac{\partial \phi_l}{\partial t}, \tag{2.2}$$

and, for the exterior motion ($a < r < \infty$),

$$\nabla^2 \phi_a = 0, \tag{2.3}$$

$$p_a = -\rho_a \frac{\partial \phi_a}{\partial t}. \tag{2.4}$$

where ϕ is the velocity potential and p is the pressure disturbance. For irrotational motion, the boundary conditions at the interface require the continuity of the radial velocity and the balance of the normal stresses by interfacial tension. For small departures about the spherical shape, $a >> \zeta$ and the boundary conditions can be written as

$$u_r^l = u_r^a, \tag{2.5}$$

for the continuity of the radial velocity at $r = a$ and

$$\left[\left[-p + 2\mu \frac{\partial u_r}{\partial r}\right]\right] = \frac{\gamma}{a^2}(L^2 - 2)\zeta, \tag{2.6}$$

for the balance of normal stresses across the interface $r = a$, written in linearized form, accounting for the pressure balance in the undisturbed state. The notation $[[\cdot]] = (\cdot)_{r=b^+} - (\cdot)_{r=b^-}$ is being used to denote the jump across the interface located at $r = a$. The linearized kinematic condition is

$$u_r = \frac{\partial \zeta}{\partial t}, \tag{2.7}$$

at $r = a$ with, $u_r = \partial\phi/\partial r$. The right-hand side of (2.6) is obtained from the linearized form of the divergence of the outward unit normal vector to the disturbed interface for the interior fluid. The operator L^2 is also known as the spherical Laplacian and emerges, for instance, in the solution of the Laplace equation using spherical coordinates by applying the method of separation of variables. It is defined as

$$-L^2\zeta = \frac{1}{\sin\theta}\frac{\partial}{\partial\theta}\left(\sin\theta\frac{\partial\zeta}{\partial\theta}\right) + \frac{1}{\sin^2\theta}\frac{\partial^2\zeta}{\partial\varphi^2}. \tag{2.8}$$

Solutions of (2.1) and (2.3) for the interior and exterior of a sphere, respectively, can be sought in the form

$$\phi_l(r,\theta,\varphi,t) = \sum_{\ell=0}^{\infty} A_\ell \left(\frac{r}{a}\right)^\ell e^{-\sigma_\ell t} S_\ell(\theta,\varphi) + \text{c.c.} \qquad 0 \le r < a, \tag{2.9}$$

$$\phi_a(r,\theta,\varphi,t) = \sum_{\ell=0}^{\infty} C_\ell \left(\frac{r}{a}\right)^{-\ell-1} e^{-\sigma_\ell t} S_\ell(\theta,\varphi) + \text{c.c.} \qquad a < r < \infty, \tag{2.10}$$

such that ϕ_l is finite at $r = 0$ and ϕ_a remains bounded as $r \to \infty$; σ_ℓ is an eigenvalue to be determined. It will be shown that σ_ℓ does not depend upon the index m. The symbol c.c. designates the complex conjugate of the previous term. The functions S_ℓ are the surface harmonics of integral order

$$S_\ell(\theta,\varphi) = \sum_{m=-\ell}^{\ell} B_{\ell m} Y_\ell^m(\theta,\varphi), \tag{2.11}$$

which, with the choice $\bar{B}_{\ell m} = B_{\ell,-m}$, are real functions. The functions $Y_\ell^m(\theta,\varphi)$ are known as the spherical harmonics (Strauss 1992)

$$Y_\ell^m(\theta,\varphi) = P_\ell^{|m|}(\cos\theta)e^{im\varphi}, \tag{2.12}$$

where $P_\ell^{|m|}$ are the associated Legendre functions. The spherical harmonics satisfy

$$L^2 Y_\ell^m(\theta,\varphi) = \ell(\ell+1)Y_\ell^m(\theta,\varphi), \tag{2.13}$$

for $\ell = 0, 1, 2, \ldots$ and $m = -\ell, \ldots, -1, 0, 1, \ldots, \ell$. The operator L^2 has been defined in (2.8). Expressions for the radial components of the velocity can be obtained from (2.9) and (2.10) by applying $u_r = \partial\phi/\partial r$. Then, the pressure disturbances p_l and p_a can be obtained from (2.2) and (2.4).

Let us write the disturbance of the spherical shape of the interface as a series expansion,

$$\zeta(\theta,\varphi,t) = \sum_{\ell=0}^{\infty} \zeta_\ell(\theta,\varphi)\mathrm{e}^{-\sigma_\ell t} + \text{c.c.}. \tag{2.14}$$

By considering $\zeta_\ell(\theta,\varphi) = \zeta_{0\ell} S_\ell(\theta,\varphi)$, where $\zeta_{0\ell}$ is a constant, and using conditions (2.5) and (2.7) one obtains

$$-\sigma_\ell\zeta_{0\ell} = \left(\frac{\ell}{a}\right) A_\ell, \qquad \sigma_\ell\zeta_{0\ell} = \left(\frac{\ell+1}{a}\right) C_\ell. \tag{2.15}$$

In addition, we have

$$(L^2-2)\zeta=\sum_{\ell=0}^{\infty}\{\ell(\ell+1)-2\}\zeta_{0\ell}\mathrm{e}^{-\sigma_\ell t}S_\ell+\text{c.c.}=\sum_{\ell=0}^{\infty}(\ell+2)(\ell-1)\zeta_{0\ell}\mathrm{e}^{-\sigma_\ell t}S_\ell+\text{c.c.}, \tag{2.16}$$

by virtue of (2.13) and (2.14). Substituting normal-mode expressions for u_r and p, obtained using (2.9) and (2.10), into the left-hand side of (2.6), applying the result (2.16) and replacing A_ℓ and C_ℓ with (2.15) yields the dispersion relation for the eigenvalue σ_ℓ, which, after some manipulation, may be written as

$$\begin{aligned}\Big(\rho_l(\ell+1)+\rho_a\ell\Big)\sigma^2-\Big(\frac{2\mu_l}{a^2}(\ell+1)\ell(\ell-1)+\frac{2\mu_a}{a^2}(\ell+2)(\ell+1)\ell\Big)\sigma\\ +\frac{\gamma}{a^3}(\ell+2)(\ell+1)\ell(\ell-1)=0,\end{aligned} \tag{2.17}$$

for $\ell=0,1,2,\ldots$, where the subscript ℓ has been dropped from σ for convenience. Expression (2.17) may be written in dimensionless form with the following choices of dimensionless parameters (Funada & Joseph 2002),

$$\hat{l}=\frac{\rho_a}{\rho_l},\quad \hat{m}=\frac{\mu_a}{\mu_l},\quad \hat{\sigma}=\sigma\frac{a}{U}\qquad\text{with}\qquad U=\sqrt{\frac{\gamma}{\rho_l a}}, \tag{2.18}$$

In dimensionless form, expression (2.17) becomes,

$$\begin{aligned}&\Big((\ell+1)+\hat{l}\ell\Big)\hat{\sigma}_\ell^2-\frac{2}{\sqrt{J}}\left((\ell+1)\ell(\ell-1)+\hat{m}(\ell+2)(\ell+1)\ell\right)\hat{\sigma}\\ &+(\ell+2)(\ell+1)\ell(\ell-1)=0\end{aligned} \tag{2.19}$$

with a Reynolds number

$$J=\frac{\rho_l V a}{\mu_l}=Oh^2\qquad\text{with}\qquad V=\frac{\gamma}{\mu_l}, \tag{2.20}$$

where Oh is the Ohnesorge number. In other words, $J^{-1/2}$ represents a dimensionless viscosity. Therefore, the eigenvalue $\hat{\sigma}$ for viscous potential flow (VPF) can be computed from

$$\begin{aligned}\hat{\sigma}=&\frac{(\ell+1)\ell(\ell-1)+\hat{m}(\ell+2)(\ell+1)\ell}{\sqrt{J}\left((\ell+1)+\hat{l}\ell\right)}\\ &\pm\sqrt{\left[\frac{(\ell+1)\ell(\ell-1)+\hat{m}(\ell+2)(\ell+1)\ell}{\sqrt{J}((\ell+1)+\hat{l}\ell)}\right]^2-\frac{(\ell+2)(\ell+1)\ell(\ell-1)}{(\ell+1)+\hat{l}\ell}},\end{aligned} \tag{2.21}$$

which has two different real roots or two complex roots. In the former case, the interface does not oscillate and the disturbances are damped. In the latter case, $\hat{\sigma}=\hat{\sigma}_R\pm i\hat{\sigma}_I$ where the real part represents the damping coefficient while the imaginary part corresponds to the frequency of the damped oscillations.

When both fluids are considered inviscid (IPF), expression (2.21) simplifies to ($\hat{m}\to 0$ and $\sqrt{J}\to\infty$)

$$\hat{\sigma} = \pm i\sqrt{\frac{(\ell+2)(\ell+1)\ell(\ell-1)}{(\ell+1)+\hat{l}\ell}}. \tag{2.22}$$

The same expression found by Lamb (1932).

2.1 VPF results for a spherical drop

If the external fluid has negligible density and viscosity ($\hat{l} \to 0$ and $\hat{m} \to 0$), a drop surrounded by a dynamically inactive ambient fluid is obtained, in which case expression (2.21) becomes,

$$\hat{\sigma} = \frac{\ell(\ell-1)}{\sqrt{J}} \pm \sqrt{\left[\frac{\ell(\ell-1)}{\sqrt{J}}\right]^2 - (\ell+2)\ell(\ell-1)}. \tag{2.23}$$

Moreover, for an inviscid drop $\sqrt{J} \to \infty$ and (2.23) reduces to

$$\hat{\sigma}_D = \pm i\sqrt{(\ell+2)\ell(\ell-1)} = \pm i\hat{\sigma}_D^*, \tag{2.24}$$

and the drop oscillates about the spherical form. This result was also obtained by Lamb (1932), p. 475.

Using the expression obtained from VPF in (2.23), one can readily find two roots for the rate of decay as $\sqrt{J} \to 0$ in the drop (e.g., high viscosity). The relevant root on physical grounds is given by

$$\hat{\sigma} = \hat{\sigma}_D^{*2}\sqrt{J}\frac{1}{2\ell(\ell-1)}. \tag{2.25}$$

In the case $\sqrt{J} \to \infty$ (low viscosity, say), the eigenvalues are complex, and then we encounter progressive decaying waves. These eigenvalues behave as

$$\hat{\sigma} = \frac{\ell(\ell-1)}{\sqrt{J}} \pm i\hat{\sigma}_D^*. \tag{2.26}$$

2.2 VPF results for a spherical bubble

By taking $\rho_l \to 0$ and $\mu_l \to 0$ in (2.17), the eigenvalue relation for a bubble of negligible density and viscosity embedded in a liquid is obtained for VPF

$$\hat{\sigma} = \frac{(\ell+2)(\ell+1)}{\sqrt{J}} \pm \sqrt{\left[\frac{(\ell+2)(\ell+1)}{\sqrt{J}}\right]^2 - (\ell+2)(\ell+1)(\ell-1)}, \tag{2.27}$$

where J is defined in terms of the liquid properties. In the limit of an inviscid external fluid $\sqrt{J} \to \infty$ in (2.27) and we obtain

$$\hat{\sigma}_B = \pm i\sqrt{(\ell+2)(\ell+1)(\ell-1)} = \pm i\hat{\sigma}_B^*, \tag{2.28}$$

and the bubble oscillates about the spherical shape without damping. This expression was obtained by Lamb (1932).

The dispersion relation obtained from VPF in (2.27) can be used to study the trend followed by the disturbances when $\sqrt{J} \to 0$ in the case of the bubble. In this case, monotonically decaying waves are predicted with decay rate

$$\hat{\sigma} = \hat{\sigma}_B^{*2}\sqrt{J}\frac{1}{2(\ell+2)(\ell+1)}. \tag{2.29}$$

In the case of $\sqrt{J} \to \infty$, VPF analysis for the bubble yields

$$\hat{\sigma} = \frac{(\ell+2)(\ell+1)}{\sqrt{J}} \pm i\hat{\sigma}_B^{*}. \tag{2.30}$$

Therefore, progressive decaying waves are found.

3 Dissipation approximation

Viscous effects can be included for irrotational motion through the dissipation method; neither vortical layers nor pressure corrections enter into the analysis. This method stems from the evaluation of the mechanical energy equation on the fluid domain. In this equation, the viscous dissipation in the bulk of the liquid is approximated by potential flow, while the continuity of tangential stress is enforced at the gas-liquid interface; the shear stress is put to zero (the gas being considered of negligible density and viscosity). Lamb (1932) found the exact solution for the decay rate of free gravity waves in complete agreement with the decay rate from the dissipation method for small viscosity. Lamb (1932) also used the dissipation method to compute the decay rate for small progressive waves in the free surface of a liquid spherical drop immersed in gas and a spherical bubble surrounded by liquid. The dissipation method was used by Wang *et al.* (2005a, 2005b) to predict the growth rate of capillary instability. Here, the procedure described in their work is applied to the spherical geometry. Our result goes further than Lamb's, since the effect of viscosity in the frequency of the oscillations is predicted in the analysis that follows.

3.1 Dissipation approximation for a spherical drop

In the case of a liquid drop surrounded by a vacuum, the mechanical energy equation can be written as

$$\frac{d}{dt}\int_V \rho\frac{|\boldsymbol{u}|^2}{2}\mathrm{d}V = \int_A \boldsymbol{n}\cdot\boldsymbol{T}\cdot\boldsymbol{u}\mathrm{d}A - \int_V 2\mu\boldsymbol{D}:\boldsymbol{D}\mathrm{d}V, \tag{3.1}$$

where V is the volume of the liquid sphere of radius a in the linearized problem; A is the surface of the drop and $\boldsymbol{n}$ is the unit outward normal; $\boldsymbol{u}$ is the velocity field; $\boldsymbol{T}$ is taken as the stress tensor for Newtonian incompressible flow and $\boldsymbol{D}$ is the strain-rate tensor. The last term in (3.1) represents the viscous dissipation. For potential flow, the following identity holds,

$$\int_V 2\mu \boldsymbol{D} : \boldsymbol{D} \mathrm{d}V = \int_A \boldsymbol{n} \cdot 2\mu \boldsymbol{D} \cdot \boldsymbol{u} \mathrm{d}A. \tag{3.2}$$

Therefore, (3.1) becomes,

$$\frac{d}{dt} \int_V \rho \frac{|\boldsymbol{u}|^2}{2} \mathrm{d}V = \int_A [(-p + \tau_{rr}) u_r + \tau_{r\theta} u_\theta + \tau_{r\varphi} u_\varphi] \mathrm{d}A - \int_A \boldsymbol{n} \cdot 2\mu \boldsymbol{D} \cdot \boldsymbol{u} \mathrm{d}A. \tag{3.3}$$

At the free surface $r = a$, we recall that the normal stress balance gives rise to,

$$-p + \tau_{rr} = -\frac{\gamma}{a^2}(L^2 - 2)\zeta. \tag{3.4}$$

The zero-shear-stress condition is enforced at the free surface

$$\tau_{r\theta} = 0, \qquad \tau_{r\varphi} = 0. \tag{3.5}$$

With these boundary conditions, the mechanical energy equation (3.3) can be expressed as

$$\frac{d}{dt} \int_V \rho \frac{|\boldsymbol{u}|^2}{2} \mathrm{d}V = -\int_A \frac{\gamma}{a^2}(L^2 - 2)\zeta u_r \mathrm{d}A - \int_A \boldsymbol{n} \cdot 2\mu \boldsymbol{D} \cdot \boldsymbol{u} \mathrm{d}A. \tag{3.6}$$

With $|\boldsymbol{u}|^2 = u_r^2 + u_\theta^2 + u_\varphi^2$ and the components of $\boldsymbol{D}$ expressed in spherical coordinates, the integrals in (3.6) can be evaluated using the formulae collected in the Appendix. These formulae become helpful to work out the integrals involving complex variables resulting from the definition of the velocity potential in §2 as the sum of a complex number plus its conjugate. The components of $\boldsymbol{u}$ and $\boldsymbol{D}$ in spherical coordinates are found from standard expressions for a Newtonian fluid. Then, carrying out the integrals in (3.6) yields

$$\begin{aligned} \frac{d}{dt} \int_V \rho \frac{|\boldsymbol{u}|^2}{2} \mathrm{d}V = & \sum_{\ell=0}^{\infty} \sum_{m=0}^{\ell} F_{\ell m} 4\pi a \rho \left(A_\ell e^{-\sigma_\ell t} + \bar{A}_\ell e^{-\bar{\sigma}_\ell t} \right) \\ & \left(-\sigma_\ell A_\ell e^{-\sigma_\ell t} - \bar{\sigma}_\ell \bar{A}_\ell e^{-\bar{\sigma}_\ell t} \right) \frac{\ell}{2\ell + 1} \frac{(\ell + m)!}{(\ell - m)!}, \end{aligned} \tag{3.7}$$

$$\begin{aligned} \int_A \frac{\gamma}{a^2}(L^2 - 2)\zeta u_r \mathrm{d}A = & \sum_{\ell=0}^{\infty} \sum_{m=0}^{\ell} F_{\ell m} 4\pi \frac{\gamma}{a^2} \left(A_\ell e^{-\sigma_\ell t} + \bar{A}_\ell e^{-\bar{\sigma}_\ell t} \right) \\ & \left(-\frac{A_\ell}{\sigma_\ell} e^{-\sigma_\ell t} - \frac{\bar{A}_\ell}{\bar{\sigma}_\ell} e^{-\bar{\sigma}_\ell t} \right) \frac{(\ell + 2)\ell^2(\ell - 1)}{2\ell + 1} \frac{(\ell + m)!}{(\ell - m)!}, \end{aligned} \tag{3.8}$$

and

$$\int_A \boldsymbol{n} \cdot 2\mu \boldsymbol{D} \cdot \boldsymbol{u} \mathrm{d}A = \sum_{\ell=0}^{\infty} \sum_{m=0}^{\ell} F_{\ell m} \frac{8\pi\mu}{a} \left(A_\ell e^{-\sigma_\ell t} + \bar{A}_\ell e^{-\bar{\sigma}_\ell t} \right)^2 \ell(\ell - 1) \frac{(\ell + m)!}{(\ell - m)!}. \tag{3.9}$$

Substitution into (3.6) yields (dropping the subscript ℓ),

$$-\left(\sigma A e^{-\sigma t}+\bar{\sigma}\bar{A}e^{-\bar{\sigma}t}\right)=\frac{\gamma}{\rho a^3}\left(\frac{A}{\sigma}e^{-\sigma t}+\frac{\bar{A}}{\bar{\sigma}}e^{-\bar{\sigma}t}\right)(\ell+2)\ell(\ell-1)$$
$$-\frac{2\nu}{a^2}\left(Ae^{-\sigma t}+\bar{A}e^{-\bar{\sigma}t}\right)(2\ell+1)(\ell-1), \tag{3.10}$$

which has the form,

$$\left[-\sigma+\frac{2\nu}{a^2}(2\ell+1)(\ell-1)-\frac{\gamma}{\rho a^3\sigma}(\ell+2)\ell(\ell-1)\right]Ae^{-\sigma t}+\text{c.c.}=0. \tag{3.11}$$

Therefore, the dissipation approximation gives rise to the dispersion relation

$$\sigma^2-\frac{2\nu}{a^2}(2\ell+1)(\ell-1)\sigma+\frac{\gamma}{\rho a^3}(\ell+2)\ell(\ell-1)=0. \tag{3.12}$$

In dimensionless form, this expression becomes,

$$\hat{\sigma}^2-\frac{2}{\sqrt{J}}(2\ell+1)(\ell-1)\hat{\sigma}+(\ell+2)\ell(\ell-1)=0. \tag{3.13}$$

where the dimensionless parameter $\hat{\sigma}$ and J have been defined in (2.18) and (2.20), respectively. The eigenvalues are

$$\hat{\sigma}=\frac{(2\ell+1)(\ell-1)}{\sqrt{J}}\pm\sqrt{\left[\frac{(2\ell+1)(\ell-1)}{\sqrt{J}}\right]^2-(\ell+2)\ell(\ell-1)}, \tag{3.14}$$

which has two different real roots or a complex-conjugate pair of roots. For $\text{Im}(\hat{\sigma})=0$, the monotonic decay rate for standing waves is obtained. In the case of progressive waves ($\text{Im}(\hat{\sigma})\neq 0$), the rate of decay $(2\ell+1)(\ell-1)/\sqrt{J}$ was obtained by Lamb (1932) in §355 through the dissipation method. In the present calculations, the relation (3.14) also gives rise to viscous effects in the frequency of the oscillations, which determine the crossover from the progressive-wave regime to the standing-wave regime. Such effects were not predicted by Lamb's dissipation method. Hence, no crossover from progressive waves to standing ones can be obtained from his calculation. Expression (3.14) can be compared with (2.23) from VPF and (2.24) from IPF.

As $\sqrt{J}\to 0$, (3.14) produces two real roots for the rate of decay; the following gives the lowest rate of decay,

$$\hat{\sigma}=\hat{\sigma}_D^{*2}\sqrt{J}\frac{1}{2(2\ell+1)(\ell-1)}. \tag{3.15}$$

In the case of $\sqrt{J}\to\infty$ the eigenvalues are complex,

$$\hat{\sigma}=\frac{(2\ell+1)(\ell-1)}{\sqrt{J}}\pm i\hat{\sigma}_D^{*}. \tag{3.16}$$

Hence, one finds progressive decaying waves. The definition of $\hat{\sigma}_D^*$ is given in (2.24).

Prosperetti (1977) studied the initial value problem posed by small departures from the spherical shape of a viscous drop surrounded by another viscous liquid. In the case of a drop

in a vacuum, he found (3.14) in the limit $t \to 0$ if an irrotational initial condition is assumed. We remark that (3.14) was obtained here by a different method.

3.2 Dissipation approximation for a spherical bubble

Following the same steps as those described for the drop, the dispersion relation for a spherical bubble immersed in liquid can also be obtained from the dissipation method. In this case, the eigenvalues are

$$\hat{\sigma} = \frac{(2\ell+1)(\ell+2)}{\sqrt{J}} \pm \sqrt{\left[\frac{(2\ell+1)(\ell+2)}{\sqrt{J}}\right]^2 - (\ell+2)(\ell+1)(\ell-1)}, \tag{3.17}$$

with J determined from the liquid properties. In the case of progressive waves, the rate of decay given in (3.17) as $(2\ell+1)(\ell+2)/\sqrt{J}$ is the same as the rate computed by Lamb (1932) using the dissipation method without the explicit inclusion of the surface tension effects in the formulation.

Expression (3.17) yields the following result as $\sqrt{J} \to 0$ ($\nu \to \infty$, say) for the bubble,

$$\hat{\sigma} = \hat{\sigma}_B^{*2}\sqrt{J}\frac{1}{2(2\ell+1)(\ell+2)}, \tag{3.18}$$

and thus monotonically decaying waves with $\hat{\sigma}_B^*$ defined in (2.28).

In the case of $\sqrt{J} \to \infty$ ($\nu \to 0$, say), the dissipation method predicts progressive decaying waves with eigenvalues

$$\hat{\sigma} = \frac{(2\ell+1)(\ell+2)}{\sqrt{J}} \pm i\hat{\sigma}_B^*. \tag{3.19}$$

4 Exact solution of the linearized fully viscous problem

In this section we summarize the results from the solution of the linearized equations of motion without the assumption of irrotational flow for a drop immersed in a vacuum and a bubble of negligible density and viscosity embedded in a viscous liquid. The result for the drop was presented by Reid (1960) whereas the solution for the bubble can be obtained following a similar path. In both cases, the dispersion relation coincides with the corresponding limiting results presented by Miller and Scriven (1968) and Prosperetti (1980a), who posed and solved the most general two-fluid problem. The predictions from these dispersion relations are compared with results from the irrotational approximations in §5.

The linearized Navier-Stokes equations govern this problem

$$\rho\frac{\partial \boldsymbol{u}}{\partial t} = -\nabla p + \mu\nabla^2\boldsymbol{u}, \tag{4.1}$$

with $\nabla \cdot \boldsymbol{u} = 0$ in $0 \le r < a$ for the drop and in $a < r < \infty$ for the bubble. Continuity of shear stresses at $r = a$ is satisfied.

4.1 Exact solution for a spherical drop

Reid (1960) obtained the dispersion relation for the eigenvalue σ

$$\alpha^4 = 2q^2\,(\ell-1)\left[\ell + (\ell+1)\,\frac{q - 2\ell Q^J_{\ell+1/2}}{q - 2Q^J_{\ell+1/2}}\right] - q^4, \tag{4.2}$$

with

$$Q^J_{\ell+1/2}(q) = J_{\ell+3/2}(q)/J_{\ell+1/2}(q), \qquad \alpha^2 = \frac{\sigma^*_D a^2}{\nu} = \hat{\sigma}^*_D\sqrt{J}, \qquad \frac{q^2}{\alpha^2} = \frac{\sigma}{\sigma^*_D} = \frac{\hat{\sigma}}{\hat{\sigma}^*_D}, \tag{4.3}$$

where σ^*_D is the frequency of oscillations from inviscid potential flow (IPF) given in (2.24). A thorough discussion on the solution of (4.2) is presented by Chandrasekhar (1959, 1961) when q is real. Considering ℓ fixed, the right-hand side of (4.2) is a function of q, $\Phi(q)$ say. On the axis of positive q, there is an infinite number of intervals where $\Phi(q)$ is positive. The first of these intervals, which contains $q = 0$, encloses a maximum ($\alpha^2_{\max}$). For $\alpha^2 < \alpha^2_{\max}$ this first interval gives two real roots of (4.2), which determine the slowest rate of decay. Since $\alpha^2 = \hat{\sigma}^*_D\sqrt{J}$, for every mode ℓ, the magnitude of J defines the roots. In the other intervals, one also has $0 \le \Phi(q) < \infty$. When $\alpha^2 > \alpha^2_{\max}$, (4.2) admits complex-conjugate eigenvalues with positive real parts which give the lowest rate of decay; these waves oscillate as they decay.

As $J \to 0$, the rate of decay from the exact solution of a drop surrounded by gas behaves as

$$\hat{\sigma} = \hat{\sigma}^{*2}_D\sqrt{J}\frac{2\ell+1}{2(\ell-1)(2\ell^2+4\ell+3)}. \tag{4.4}$$

From the exact solution (4.2), the trend of the complex eigenvalue $\hat{\sigma}$ for the drop as $\sqrt{J} \to \infty$ was presented by Chandrasekhar (1959, 1961) and Miller and Scriven (1968) and follows the same result (3.16) from the dissipation method.

4.2 Exact solution for a spherical bubble

A procedure similar to the one applied to the drop gives rise to the following dispersion relation for the bubble

$$\alpha^4 = (\ell+2)\,q^2\frac{(2\ell+1)\,q^2 - 2\,(\ell+1)\,(\ell-1)\left[(2\ell+1) - qQ^H_{\ell+1/2}\right]}{(2\ell+1) + q^2/2 - qQ^H_{\ell+1/2}} - q^4, \tag{4.5}$$

with

$$Q^H_{\ell+1/2} = H^{(1)}_{\ell+3/2}(q)/H^{(1)}_{\ell+1/2}(q), \tag{4.6}$$

and α^2 and q given in (4.3). In these relations, σ^*_B from IPF given in (2.28) for a bubble is used instead of σ^*_D.

Expression (4.5) is the same dispersion relation found by Miller & Scriven (1968). This dispersion relation only admits complex roots as a consequence of the character of the Hankel

functions (Prosperetti 1980a). Therefore, for a bubble, only progressive decaying waves are predicted. For a drop, we recall that real eigenvalues can be found.

For a gas bubble in a viscous liquid, a real σ can be approximated as $\sqrt{J} \to 0$,

$$\hat{\sigma} = \hat{\sigma}_B^{*2} \sqrt{J} \frac{2\ell + 1}{2(2\ell^2 + 1)(\ell + 2)}, \tag{4.7}$$

For $\sqrt{J} \to \infty$ (4.5) yields the same expression (3.19) obtained with the dissipation method. These results for small and large J were presented by Miller & Scriven (1968).

5 Results and Discussion

In this section, the comparison of the results for the decay rate and frequency of the waves according to viscous potential flow (VPF) and the dissipation method (DM) with the exact solutions of the fully viscous linear problem are presented for a drop and a bubble. A wide interval is selected for the mode number ℓ starting with $\ell = 2$. The smallest value of $\ell = 2$ is chosen since lower values yield compressive or expansive motions of the drop interface which are not compatible with the incompressibility assumption or a non-physical static disturbed interface. For higher values of ℓ, the exact fully viscous solution for the drop predicts oscillations that decay faster (Miller & Scriven 1968). The same lowest value of $\ell = 2$ is selected for the bubble case.

Figure 1(a) shows the critical Reynolds number J_c as a function of ℓ for a drop. The number J_c is defined as the value of J at a given ℓ for which transition from monotonically decaying waves (standing waves) to progressive waves (oscillations) occurs. For $J \leq J_c$ the eigenvalues $\hat{\sigma}$ are real and monotonically decaying waves take place, whereas for $J > J_c$ the eigenvalues are complex and the waves decay through oscillations. For systems with $J < 0.5$, the viscous theories predict monotonically decaying waves for a drop and for all modes. Figure 1(b) presents the trends of J_c with ℓ for VPF and DM for a bubble. Recall that the exact solution always predicts decaying oscillations (i.e. complex eigenvalues) in the bubble case. Therefore, the exact solution does not give rise to a critical J. If DM predicts progressive decaying waves, then VPF gives the same outcome. If VPF predicts standing waves, then the same behavior is obtained from DM. The viscous irrotational theories give rise to monotonically decaying waves for a bubble with $J < 10$ and for all modes.

For a drop, the decay rate and wave frequency as a function of J are presented in Figures 2(a) and (b), respectively, for $\ell = 2$ as predicted by VPF, DM and the exact solution. The wave frequency given by IPF is also included for comparison. For large J, DM and the exact solution show excellent agreement, whereas VPF is off the mark as anticipated from the comparison of (2.26) with (3.16). The wave frequencies from the three viscous theories tend to the inviscid solution for large J. As J decreases (below $J = 10$, say), transition from the progressive-wave regime to the standing-wave regime occurs. In the point of transition, the frequency becomes identically zero and the curve of the rate of decay bifurcates yielding two real and different roots. In Figure 2, the eigenvalue $\hat{\sigma}_1$, representing the least damped mode of decay, is plotted. For small J, DM approximates the exact decay rate with a discrepancy of 20%, nearly. Figures 2(a) and (b) reveal that the viscous irrotational theories qualitatively follow the trend described

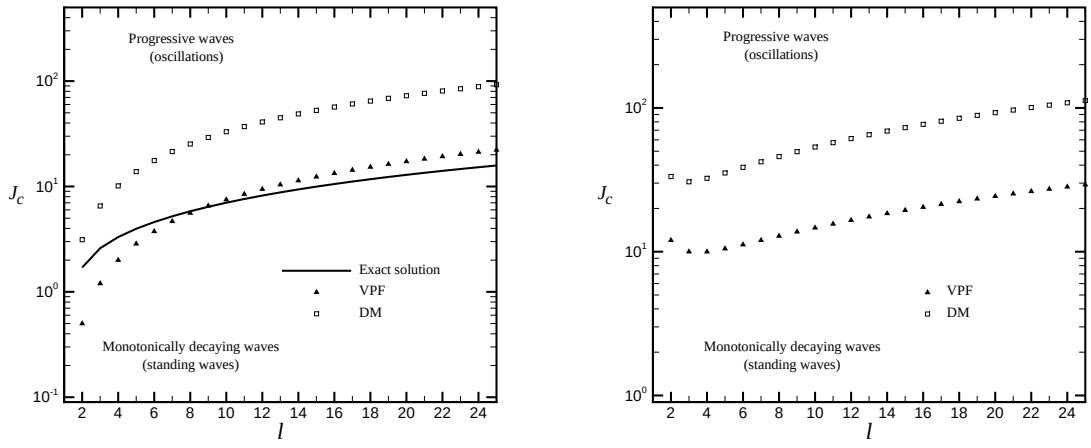

(a) drop (b) bubble

Fig. 1. Critical Reynolds number J_c as a function of the mode number ℓ for a *drop* and a *bubble*.

by the exact solution and are able to predict a progressive-to-standing-wave crossover J_c by considering viscous effects in the frequency.

For a bubble, the rate of decay and wave frequency are presented in Figures 2(c) and (d), respectively for $\ell = 2$. Notice that the rate of decay follows somewhat similar trends as those described for the drop. For small J, VPF shows the lowest discrepancy, of nearly 40%, with the exact rate of decay. Figure 2(d) shows that the exact solution does not predict transition to the standing-wave regime, but the wave frequency tends smoothly to zero as J decreases (the viscosity increases, say). On the other hand, VPF and DM do render a crossover J_c for which transition to monotonically decaying waves occurs.

For large values of J, if one of the fluids has negligible density and viscosity, a thin boundary layer results (Miller & Scriven 1968). Thus, an irrotational velocity field works as a good approximation. In terms of the dissipation approximation, such a thin boundary layer yields a negligible contribution to the total viscous dissipation, which is thus determined by the irrotational flow over the interior of the fluid domain. At the free surface, however, the zero-shear-stress condition is enforced in the formulation. Indeed, expression (3.16) and the results in §4.1 demonstrate that the dissipation method is a first order approximation to the exact solution in the dimensionless viscosity, $\epsilon \equiv J^{-1/2}$ say. By contrast, as ϵ decreases (e.g., the liquid viscosity increases), the boundary layer becomes thicker and the performance of the dissipation method deteriorates as the difference for the higher order terms in ϵ between DM and the exact solution becomes significant. A non-negligible boundary layer flow contributes substantially to the rate of viscous dissipation, hence the rate of decay increases. However, the increasing trend of the rate of decay is reversed as J continues decreasing because the motion for small J, as discussed by Prosperetti (1980a), is restrained in such a drastic way that the energy dissipation per unit time, and thus the decay rate, has to decrease as J goes to zero. In the case of the drop, the progressive-to-standing-wave crossover sharply represents this change in the trend of the decay rate.

For a bubble [Figure 2(c)], oscillatory decaying waves are always predicted by the exact linearized theory yet the smooth region where the decay-rate graph reaches a maximum as a

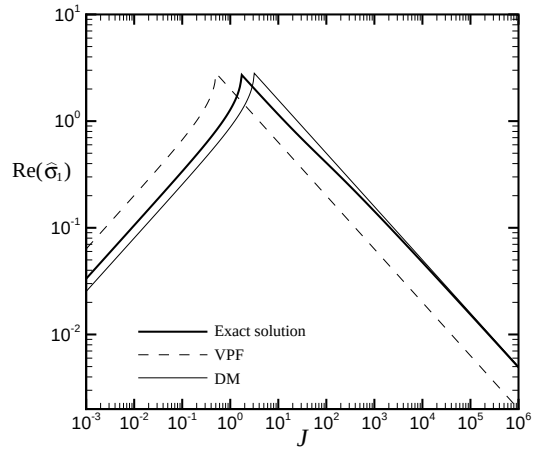

(a) Decay rate - *drop*

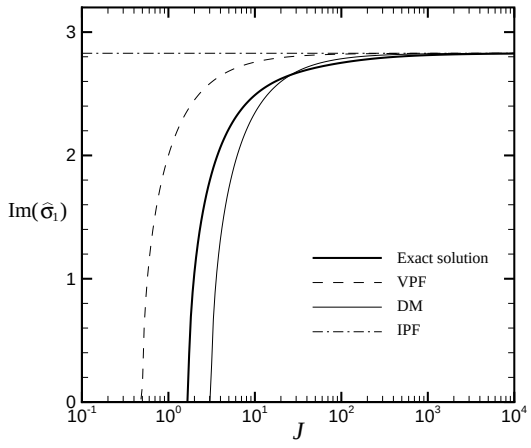

(b) Wave frequency - *drop*

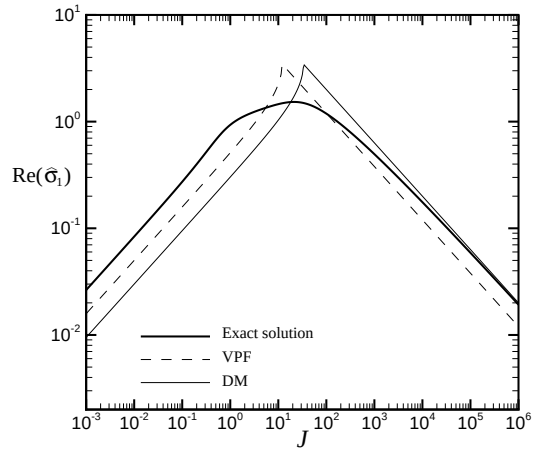

(c) Decay rate - *bubble*

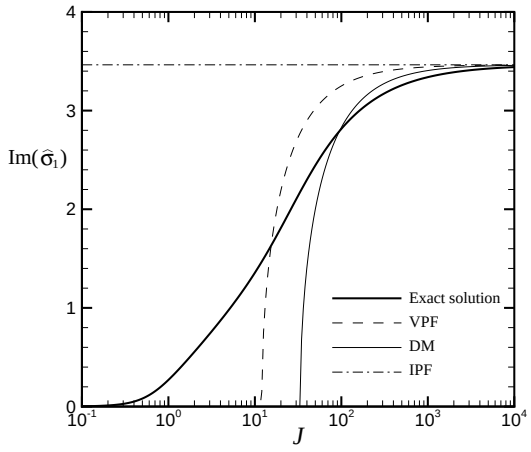

(d) Wave frequency - *bubble*

Fig. 2. Decay rate $\mathrm{Re}(\hat{\sigma}_1)$ and wave frequency $\mathrm{Im}(\hat{\sigma}_1)$ for the fundamental mode $\ell = 2$ as function of the Reynolds number J for a *drop* and a *bubble* from the exact solution, VPF, DM and IPF. The decay rate predicted by IPF is identically zero for all ℓ.

function of J suggests a transition in the structure of the flow that follows on the lines explained above.

Computations carried out for several higher modes ($\ell = 3$, 4 and 10) have shown that the features commented for the fundamental mode are also observed for these other modes (not plotted here). The general trend is that the rate of decay increases with increasing ℓ. The analysis of the predictions from the exact solution indicates that the change-over from progressive waves to standing waves takes place for a larger critical J as ℓ increases for a drop. Even though no transition to standing waves occur for the bubble, the interval of J for which very low frequencies are obtained becomes wider as ℓ increases. These results show that viscosity damps the motion more effectively for shorter waves. The viscous irrotational theories follow these tendencies.

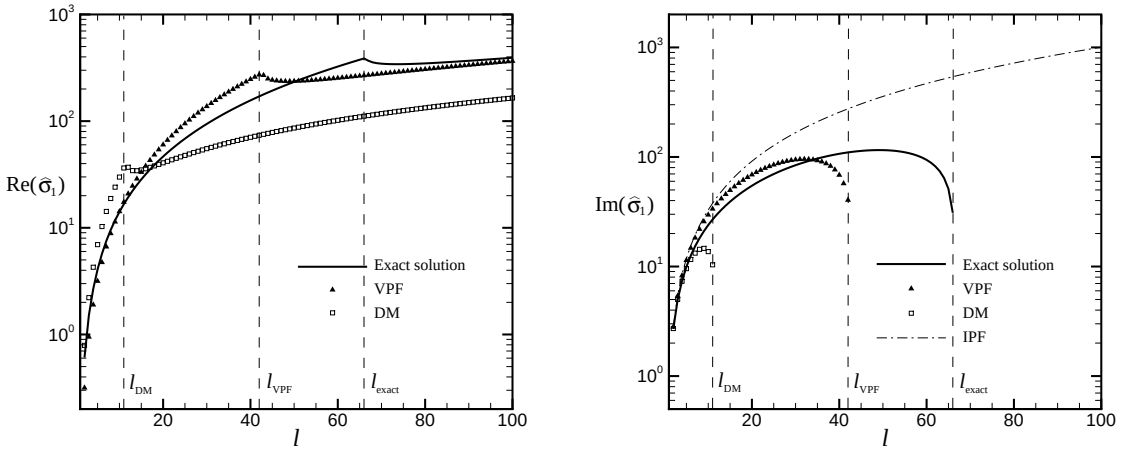

(a) Decay rate (b) Wave frequency

Fig. 3. Decay rate $\mathrm{Re}(\hat{\sigma}_1)$ and wave frequency $\mathrm{Im}(\hat{\sigma}_1)$ for $J = 40$ versus the mode number ℓ for a *drop*. In this case, the eigenvalues are a pair of complex conjugates for the interval of $\ell \leq \ell_{\mathrm{c}}$ and they are real and different for $\ell > \ell_{\mathrm{c}}$. For the latter case, the lowest decay rate is plotted in (a). The symbol ℓ_{c} stands for the highest value of ℓ for which a non-zero imaginary part is obtained, i.e. progressive waves occur. For instance, $\ell_{\mathrm{c}} = \ell_{\mathrm{exact}}$ from the exact solution.

For a drop, when $J << 1$ in the standing-wave regime, VPF shows good agreement with the exact solution for short waves or large ℓ (not plotted). This tendency can be anticipated from (2.25) and (4.4). The same response is observed for a bubble. In the case of large mode number ℓ, the dynamics of the short waves may be modeled as small disturbances about a horizontal, plane free surface. This problem was solved by Lamb (1932) §349. For large viscosity (i.e. small $\sqrt{J}$), he argues that the least damped mode 'represents a slow creeping of the fluid towards a state of equilibrium with a horizontal surface'. From Lamb's analysis, it is clear that this flow is nearly irrotational, thus explaining the good agreement between VPF and the exact solution.

As J increases, waves of certain length becomes oscillatory waves. For instance, in the case of $J = 40$ shown in Figure 3 , the crossover values of ℓ according to every viscous theory enters into the analysis. In this case, progressive waves exist according to the viscous theories for $\ell < \ell_{\mathrm{DM}}$, whereas these theories agree and predict standing waves for $\ell > \ell_{\mathrm{exact}}$. For large J, the crossover ℓ_c obtained from each viscous theory may also be large (e.g., $\ell_c > 100$ for $J = 10^6$), since viscous effects are weak and short waves oscillate. In the regime of progressive waves, $\ell \leq \ell_c$, there exists a region of good agreement between DM and the exact solution that extends to higher values of $\ell \geq 2$, while VPF shows poor agreement in comparison. At least for values of $\ell << \ell_{exact}$ in the neighborhood of $\ell = 2$, DM provides the better approximation of the decay rate for the drop or the bubble.

Concluding remarks

The results obtained from the viscous purely irrotational approximations for the decay rate and frequency of the oscillations for a drop and a bubble follow the trends described by the exact solution, showing qualitative agreement with most of the features depicted by this theory. The damping role of viscosity in the dynamics of the waves is adequately described by the viscous

irrotational theories through the modeling of the decay rate and frequency of the oscillations, in contrast to the classical inviscid theory, which predicts undamped oscillations. Quantitative agreement is also demonstrated for certain intervals of modes and dimensionless viscosity. Some notable features from the comparison carried out in this study for the drop and the bubble are:

- In the case of short waves (i.e. large mode number ℓ) and large viscosity, VPF gives a very good approximation of the waves' decay rate for both the drop and the bubble. On the other hand, the dissipation method gives rise to values of the decay rate in closer agreement with the exact solution within a certain ℓ interval, including $\ell = 2$, in the progressive-wave regime (i.e. long waves) for large values of the Reynolds number J or small viscosity. This trend resembles the tendencies obtained for free gravity waves perturbing a plane interface by Wang & Joseph (2006). Nonetheless, a notable difference between their results and those given here is that surface tension has a stronger regularizing effect on short waves than gravity.
- VPF approximates the variation of frequency with the mode number with the lowest discrepancy for a fixed J. In particular, the transition from progressive to standing waves predicted by this irrotational theory occurs at a higher critical value of ℓ than the threshold given by the dissipation method.
- The viscous irrotational approximations predict effects of viscosity on the frequency of the oscillations. For every mode, there exists a J for which transition from progressive waves to monotonically decaying waves occurs for either the drop or the bubble. Whereas a transitional value of J is predicted by the exact solution for a drop, only progressive waves are found by this theory for a bubble. In this case, very small frequencies are obtained as $\sqrt{J} \to 0$ (e.g., $\nu \to \infty$) from the exact solution.
- The viscous irrotational theories do not give rise to a continuos spectrum of eigenvalues for the bubble as has been found for the exact solution by Prosperetti (1980a).

Acknowledgements

The work of J.C. Padrino and D.D. Joseph was partially supported by a grant 0302837 from the National Science Foundation.

References

Basaran, O. 1992 Nonlinear oscillations of viscous liquid drops. *J. Fluid Mech.* **241**, 169–198.

Bowman, J. J., Senior, T. B. A. & Uslenghi, P. L. E. (Ed.) 1987 *Electromagnetic and Acoustic Scattering by Simple Shapes*. Hemisphere Publishing Corporation, New York.

Chandrasekhar, S. 1959 *The oscillations of a viscous liquid globe*. Proc. London Math. Soc. (3), 9, 141–49.

Chandrasekhar, S. 1961 *Hydrodynamic and Hydromagnetic Stability*. Oxford University Press.

Funada, T. & Joseph, D. D. 2002 Viscous potential flow analysis of capillary instability. *Int. J. Multiphase Flow* **28**, 1459–1478.

Joseph, D. D. 2003 Viscous potential flow. *J. Fluid Mech.* **479**, 191–197.

Joseph, D. D. 2006 Potential flow of viscous fluids: Historical notes. *Int. J. Multiphase Flow* **32**, 285–310.

Joseph, D. D. & Liao, T.Y. 1994a Potential flows of viscous and viscoelastic fluids. *J. Fluid Mech.* **265**, 1–23.

Joseph, D. D. & Liao, T.Y. 1994b Viscous and viscoelastic potential flow. In *Trends and Perspectives in Applied Mathematics.* vol. 100 (ed. S. Sirovich & V. Arnol'd) pp. 1–54. Springer.

Joseph, D. D. & Wang, J. 2004 The dissipation approximation and viscous potential flow. *J. Fluid Mech.* **505**, 365–377.

Lamb, H. 1881 On the oscillations of a viscous spheroid. *Proc. Lond. Math. Soc.* **13**, 51–66.

Lamb, H. 1932 *Hydrodynamics.* Sixth edition. Cambridge University Press. Reprinted by Cambridge University Press, 1993.

Lord Kelvin 1890 Oscillations of a liquid sphere, in *Mathematical and Physical Papers.* Clay and Sons, London, Vol. 3, pp. 384–386.

Lord Rayleigh 1896 *The Theory of Sound.* Second edition. MacMillan, London. Reprinted by Dover, New York, 1945. Vol. 2, p. 371.

Lundgren, T.S. & Mansour, N.N. 1988 Oscillations of drops in zero gravity with weak viscous effects. *J. Fluid Mech.* **194**, 479–510.

Miller, C. A. & Scriven, L. E. 1968 The oscillations of a fluid droplet immersed in another fluid. *J. Fluid Mech.* **32**(3), 417–435.

Patzek, T.W., Benner, R.E., Basaran, O.A. & Scriven, L.E. 1991 Nonlinear oscillations of inviscid free drops. *J. Comp. Phys.* **97**, 489–515.

Prosperetti, A. 1977 Viscous effects on perturbed spherical flows. *Quart. Appl. Math.* **35**, 339–352.

Prosperetti, A. 1980a Normal-mode analysis for the oscillations of a viscous liquid drop in an immiscible liquid. *J. Méc.* **19**, 1, 149–182.

Prosperetti, A. 1980b Free oscillations of drops and bubbles: the initial value problem. *J. Fluid Mech.* **19**, 1, 149–182.

Reid, W.H. 1960 The oscillations of a viscous liquid drop. *Quart. Appl. Math.* **18**, 86–89.

Strauss, W. A. 1992 *Partial Differential Equations: An Introduction.* John Wiley & Sons, Inc.

Tomotika, S. 1935 On the stability of a cylindrical thread of a viscous liquid surrounded by another viscous fluid. *Proc. R. Soc. Lond.* A **150**, 322–337.

Tsamopoulos, J.A. & Brown, R.A. 1983 Nonlinear oscillations of inviscid drops and bubbles. *J. Fluid Mech.* **127**, 519–537.

Valentine, R.S., Sather, N.F. & Heideger, W.J. 1965 The motion of drops in viscous media. *Chem. Eng. Sci.* **20**, 719–728.

Wang, J., Joseph, D. D. & Funada, T. 2005a Pressure corrections for potential flow analysis of capillary instability of viscous fluids. *J. Fluid Mech.* **522**, 383–394.

Wang, J., Joseph, D. D. & Funada, T. 2005b Viscous contributions to the pressure for potential flow analysis of capillary instability of two viscous fluids. *Phys. Fluids* **17**, 052105.

Wang, J., & Joseph, D. D. 2006 Purely irrotational theories of the effect of the viscosity on the decay of free gravity waves. *J. Fluid Mech.* **559**, 461–472.

A Integration formula

In performing the integration of the mechanical energy equation (3.6) in §3, the following formula is invoked,

$$\int_A \left(B+\bar{B}\right)\left(C+\bar{C}\right)\mathrm{d}A = 2\int_A \mathrm{Re}\left[BC+B\bar{C}\right]\mathrm{d}A = 2\mathrm{Re}\left[\int_A \left(BC+B\bar{C}\right)\mathrm{d}A\right], \tag{A.1}$$

where A represents either a surface or a volume and B and C are complex fields. The bar indicates complex conjugate and $\mathrm{Re}\,[\cdot]$ is a linear operator that returns the real part of a complex number.

Other formulae used to evaluate the integrals in the mechanical energy equation (3.6) correspond to standard results involving Legendre functions and Fourier series in complex form. With S_ℓ defined in (2.11), these formulae are

$$\int_0^{2\pi}\int_0^{\pi} S_\ell S_k \sin\theta \mathrm{d}\theta\mathrm{d}\varphi = \sum_{m=-\ell}^{\ell}\sum_{j=-k}^{k} B_{\ell m}\bar{B}_{kj}\int_0^{2\pi}\int_0^{\pi} P_\ell^{|m|}(\cos\theta)P_k^{|j|}(\cos\theta)e^{i(m-j)\varphi}\sin\theta\mathrm{d}\theta\mathrm{d}\varphi, \tag{A.2}$$

with S_k real (i.e. $S_k = \bar{S}_k$). This integral is zero for all the different duplets $(\ell,m)\neq(k,j)$. Then, (A.2) reduces to

$$\begin{aligned}\int_0^{2\pi}\int_0^{\pi}[S_\ell(\theta,\varphi)]^2\sin\theta\mathrm{d}\theta\mathrm{d}\varphi &= \sum_{m=0}^{\ell} 2\pi F_{\ell m}\int_0^{\pi}\left[P_\ell^m(\cos\theta)\right]^2\sin\theta\mathrm{d}\theta \\ &= \sum_{m=0}^{\ell} F_{\ell m}\left[\frac{4\pi}{2\ell+1}\frac{(\ell+m)!}{(\ell-m)!}\right],\end{aligned} \tag{A.3}$$

using a standard result for the integral in the second term. Here, $F_{\ell m}$ denotes real constants.

Another result used in the evaluation of (3.6) is

$$\begin{aligned}&\int_0^{2\pi}\int_0^{\pi}\left[\sin\theta\frac{\partial S_\ell}{\partial\theta}\frac{\partial S_k}{\partial\theta}+\frac{1}{\sin\theta}\frac{\partial S_\ell}{\partial\varphi}\frac{\partial S_k}{\partial\varphi}\right]\mathrm{d}\theta\mathrm{d}\varphi = \sum_{m=-\ell}^{\ell}\sum_{j=-k}^{k} B_{\ell m}\bar{B}_{kj} \\ &\int_0^{2\pi}\int_0^{\pi}\left[\sin\theta\frac{dP_\ell^{|m|}(\chi)}{d\theta}\frac{dP_k^{|j|}(\chi)}{d\theta}+\frac{mj}{\sin\theta}P_\ell^{|m|}(\chi)P_k^{|j|}(\chi)\right]e^{i(m-j)\varphi}\mathrm{d}\theta\mathrm{d}\varphi,\end{aligned} \tag{A.4}$$

where $\chi=\cos\theta$. This integral is also zero for all different duplets $(\ell,m)\neq(k,j)$. Otherwise, this integral reduces to (Bowman, Senior & Uslenghi 1987)

$$\begin{aligned}&\int_0^{2\pi}\int_0^{\pi}\left[\sin\theta\left(\frac{\partial S_\ell}{\partial\theta}\right)^2+\frac{1}{\sin\theta}\left(\frac{\partial S_\ell}{\partial\varphi}\right)^2\right]\mathrm{d}\theta\mathrm{d}\varphi = \sum_{m=0}^{\ell}2\pi F_{\ell m}\int_0^{\pi}\Bigg[\sin\theta\left(\frac{dP_\ell^m(\chi)}{d\theta}\right)^2 \\ &+\frac{m^2}{\sin\theta}\left(P_\ell^m(\chi)\right)^2\Bigg]\mathrm{d}\theta = \sum_{m=0}^{\ell}F_{\ell m}\left[\frac{4\pi\ell(\ell+1)}{(2\ell+1)}\frac{(\ell+m)!}{(\ell-m)!}\right].\end{aligned} \tag{A.5}$$